IPPI
Polyolefins Journal, Vol. 11, No. 2 (2024)
DOI: 10.22063/POJ.2023.3514.1283
ORIGINAL PAPER

Magnesium alkoxide precursor to Ziegler-Natta catalyst - emphasis on morphology studies through computer vision approach

Yogeshwar N Thakare, Ajay V Kothari, Saurabh Shinde, Pooja Kadam, Natarajan Venkateswaran, Virendrakumar Gupta*

Reliance Research & Development Centre, Reliance Corporate Park,
Reliance Industries Limited (RIL), Thane Belapur Road, Navi Mumbai-400701, India

Received: 12 October 2023, Accepted: 17 December 2023

ABSTRACT

$MgCl_2$-supported Ti catalyst is usually used in commercial propylene polymerization process. Morphology is a key performance determination parameter for polymer resins produced by commercial olefin polymerization process. Higher resin flowability and bulk density (greater than 0.38 g/cm^3) are demonstrated by 'good' morphological resins (sphericity close to '1'). Polymer resin morphology is controlled by morphology of the catalyst used as well as polymerization conditions. The industrially accepted approaches to control polymer resin morphology are by controlling catalyst morphology through various approaches like pre-polymerization of the catalysts. Morphology of the catalyst is dependent on precursor (support) morphology and process parameters for making the catalyst. In this work, we have developed magnesium alkoxide precursor, a Ziegler-Natta catalyst using the precursor and studied its performance in gas phase propylene polymerization process. Further, morphology of different precursor and catalyst samples is evaluated and correlated with using a "computer vision" based approach. The approach involves modeling the circularity (as an analog of sphericity) of a catalyst and precursor particle. It is observed that the circularity of catalyst particles is lower than that of precursor, due to attrition in the process, and it is also reflected in the increase in the particle size distribution span from 0.83 to 1.32 while synthesis of catalyst from precursor. This approach provides a tool to evaluate and screen the catalysts for using in polymerization.
Polyolefins J (2024) 11: 71-82

Keywords: Morphology; computer vision; catalyst; polymer; resin.

INTRODUCTION

Polymer resin with spherical morphology is ideal for smooth operation of gas phase polyolefin reactor due to good fluidization, enhanced heat and mass transfer, improved bulk density and improved resin flowability [1,2]. Non-spherical particle shows poor fluidization behavior as compared to that of spherical particles. For particles with the same volume-equivalent diameter, non-spherical particles show lower minimum fluidization velocity and fluidizing coefficient [3].

Various parameters determine the polymer resin morphology e.g., catalyst morphology, polymerization conditions and molecular organization [4-12]. Amongst all these parameters, catalyst morphology is the biggest contributor in determining polymer resin morphology [13]. Other factors such as catalyst surface area, pore size and particle size distribution affect the rate of reactants transport inside the growing particle [14-16]. It also affects overall polymerization rate and molecular architecture of the polymer such as chain length distribution, comonomer content, etc [17-18]. Morphology of the

*Corresponding Author - E-mail: virendrakumar.gupta@ril.com

Ziegler-Natta catalyst is also dependent on precursor morphology and catalyst manufacturing process. Thus, control over final polymer particle morphology can be achieved by the way of tuning precursor morphology and catalyst manufacturing conditions. Precursor morphology is controlled by precursor manufacturing process.

Broadly, there are three main approaches for synthesis of magnesium dichloride supported Ziegler-Natta catalyst i.e., ball-milling [4-6], alcohol-adduct [7-10] and magnesium alkoxide [11-12]. In the first method, magnesium chloride is used as support, it is mixed with internal electron donor by ball milling technique and is further treated with $TiCl_4$. In the other two methods, morphological precursor (i.e., alcohol-adduct and magnesium alkoxide) is reacted with $TiCl_4$ in presence of an internal donor, to have well-shaped $MgCl_2$ supported catalyst.

Mori *et al.*, in 1999 reported evolution of $MgCl_2$ structure in supported Ziegler-Natta catalyst, and observed through high resolution transmission electron microscopy [19]. They reported the effect of catalyst synthesis process on $MgCl_2$ crystal structure deformation. Ball milling approach was adopted for catalyst synthesis. Presence of an organic solvent during catalyst synthesis resulted into spherical catalyst with nearly uniform particle size distribution.

Arabi and Abedini in 2013 studied effect of reaction temperature and amount of titanium tetrachloride on the morphology of Ziegler-Natta catalyst and its polymerization performance [20]. They observed optimum catalyst activity and morphology when catalyst synthesis is carried out in two stages. They used $MgCl_2.C_2H_5OH$ adduct for catalyst synthesis. Spherical morphology of the catalyst particles was retained by gradual increases in reaction temperature. The reaction initiated at -5°C and was gradually heated to 90°C. Rapid increase in reaction temperature is reported to promote fragmentation of catalyst particles. Fragmentation leads to non-spherical and small size catalyst particles, with broader particle size distribution. Chumachenko *et al*., in 2017 studied Ziegler-Natta catalyst synthesis using solid $Mg(OEt)_2$ precursor [21]. A similar observation i.e., breakage of initial solid $Mg(OEt)_2$ leading to a broader catalyst particle size distribution, has been reported.

Ziegler-Natta catalyst can be represented by multigrain model since it is made up of many crystals of identical orientation. Redzic in 2016 studied preparation of catalysts for ethylene polymerization by precipitating $MgCl_2$ by $EtAlCl_2$, followed by subsequent treatment with $TiCl_4$ [22]. Experiments were carried out at precipitation temperature in the range of 40 to 120°C. Precipitation temperature was found to alter the thickness of the $MgCl_2$ crystal size, and characterized by XRD. They obtained largest crystals at a synthesis temperature of 60°C. Smaller crystals at higher precipitation temperature were obtained due to faster reaction rate. Whereas lower crystal size can be elucidated by slower chlorination reaction of $Mg(OR)_2$ by $EtAlCl_2$ leading to an insufficient crystal growth. The catalyst produced at lower temperature was having irregular morphology. Bigger catalyst particles with spherical morphology were obtained at higher catalyst synthesis temperatures. Reaction conditions in initial stages of polymerization plays key role in determining the polymer particle morphology. This can be overcome by pre-polymerization of the catalyst under milder conditions [23].

Several models have been reported over the years to explain the polymer particle growth mechanism. Solid core model, flow model and the multigrain model are the most popular amongst them. Polymerization reaction occurs on the solid catalyst according to the solid core model. According to the flow model, the growing polymer flows outward and accumulates outside the particle. Whereas the multigrain model assumes a catalyst composed of microparticles. Reactants diffuse inside the catalyst pores, polymerize on the microparticles, and form a polymer layer around it, leading to expansion of particle as polymerization progresses [24-25]. These models can be used for describing polymerization rate as well as property distributions by providing rate of initiation, propagation, termination, and diffusion coefficients. Such models are useful for revealing performance at an identical set of operating conditions, but it is difficult to extrapolate it for varied reaction conditions. Since morphology of a catalyst has a strong influence on polymerization performance, the model response varies for different catalyst batches, although produced under similar reaction conditions. This is because of variation in rates of intraparticle mass transfer inside varied morphology catalyst batches. Different particle internal morphologies are developed due to even small variation in reaction conditions over a short time, especially in initial stages. Predictive models need parameters tuning for fitting to specific set of reaction conditions [23]. Polymer morphology development from a catalyst is widely studied and reported, but studies on morphology replication from precursor to catalysts are rare.

Our interest in understanding the polypropylene

polymer using magnesium dichloride catalyst has led to a depth understanding of synthetic methodology, characteristics of magnesium dichloride supported catalyst process, catalyst characterization, polymerization process and also established correlation [26-28]. Our group earlier reported polypropylene resin flowability improvement through catalyst morphology [29]. Flowability of the polypropylene resin produced using morphological and non-morphological catalyst was quantified by flow time and angle of repose. Spherical catalyst yields polymer resin with good morphology, which gives better flowability. Since morphology data are in qualitative form, there is difficulty in correlations development at industrial scale. There are limited tools to convert qualitative morphology results into quantitative numbers. In the current studies, morphological variations from precursor to catalyst are quantified by computer vision approach.

Computer vision approach for particle morphology determination

Computer vision is a field of Artificial Intelligence (AI) applied to interpret and understand the visual world, with trained computers. Using digital images from cameras and videos, deep learning models can accurately identify and classify objects and react to what they "see".

Computer vision includes methods for acquiring, processing, analyzing, and understanding digital images. Understanding in this context means the transformation of visual images (the input to a human eye) into attributes from the real world that make sense to thought processes and can elicit appropriate action. This image understanding can be seen as the extraction of information from image data using models constructed with the aid of geometry, physics, statistics, and learning theory. The image data can take many forms, such as video sequences, views from multiple cameras, multi-dimensional data from a 3D scanner, etc. The discipline of computer vision is concerned with the theory enabling artificial systems to extract information from images.

A simplified illustration of how a smiley face (image) may be transformed to binary form (data) prior to be being processed is shown below:

Some areas where Computer Vision (CV) can be applied

* Image processing (e.g., Image enhancement, image reconstruction, image-based measurements)
* Object detection (e.g., Identify and recognize objects, faces, surveillance, etc.)
* Object tracking (e.g., track a moving object – soccer ball, car, etc.)
* Handwriting and signboard reading (e.g., convert handwritten notes into digital format, read vehicle number plates, etc.)
* Search engine image search (e.g., Google Lens)

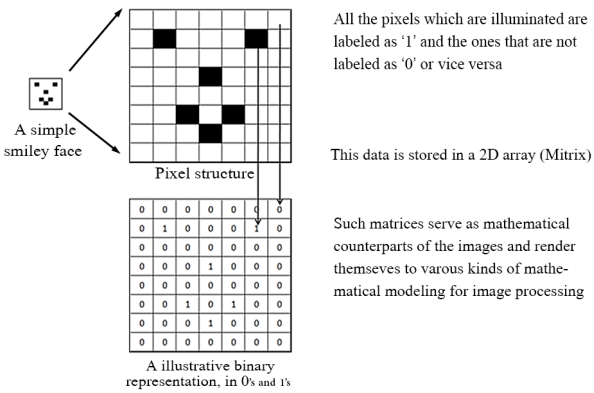

Figure 1. Image representation for analysis.

EXPERIMENTAL

Materials

Magnesium alkoxide is used as precursor for synthesis of Ziegler-Natta catalyst. Catalyst was produced by treating it with titanium tetrachloride and diisobutyl phthalate internal donor in multiple steps. Precursor and catalysts were produced at commercial scale as per process described in patents [30-32]. These catalysts were used for gas phase propylene polymerization. Four different batches of precursor and catalysts synthesized under identical conditions were selected for morphological investigations.

Particle size distribution

Particle size distribution (PSD) of the precursor and catalysts was analyzed by CILAS-1190 instrument. Mineral oil was used as circulating media for analyzing the PSD. Catalyst slurry of desired concentration was prepared in mineral oil. All the samples were sonicated for 2 min for de-agglomeration, before characterization of the particle size. Distribution of particle size is reported at 10%, 50%, 90% of the population and the mean particle size is also reported.

Span of particle size distribution (D_{span}) can be calculated as:

$$D_{span} = \frac{(D_{90} - D_{10})}{D_{50}}$$

Where, D_{10} refers to the particle size where 10% of the particles in that sample (by weight) are smaller, D_{50} refers to the particle size where 50% of the particles in that sample (by weight) are smaller and D_{90} refers to the particle size where 90% of the particles in that sample (by weight) are smaller.

Morphological characteristics

Scanning electron microscopy (SEM) of catalyst particles was performed on Inspect S (D8419) model make FEI instrument at an operation voltage of 10-15 kV at magnifications of 1000 ×. Mineral oil slurried catalyst was washed multiple times with dry hexane to make it oil free, followed by drying under inert atmosphere. The SEM images of catalyst particles were then used for analysis.

Circularity distribution analysis

We have already discussed that the sphericity of the resin particle has a bearing on the flowability of the polymer resin. In this study, since we used only two-dimensional SEM images of particles, we have assumed and studied the "circularity" of particles as an analogous but approximated property instead of particle "sphericity".

As can be seen in Figure 2, the first step was to identify each particle in the SEM image uniquely for which contour detection techniques were used. Subsequently, the center of each contour was detected followed by enclosing the contour in a close circle. The ratio of area of the object to the area of the enclosing circle served as a metric for circularity in two dimensions which can be notionally assumed (extrapolated) as being a metric of sphericity in three dimensions. A computer vision technique called watershed method was commissioned where overlapping objects posed a difficulty. The computer vision algorithm was designed to dynamically handle various zoom levels, noise as well as images that were too large or too small which could have been outliers and skewed the results. A distribution of circularity measures was drawn up from the analysis for better understanding. Statistics of the circularity distribution were computed and compared for morphologically similar particles.

RESULTS AND DISCUSSION

Magnesium alkoxide precursor, Ziegler-Natta catalyst using it and polypropylene using resultant catalyst were produced at commercial scales as per process described in patents [30-32]. The characteristics of precursor, catalyst and polypropylene are mentioned in the following section:

Precursor, catalyst, polypropylene synthesis and performance

Magnesium alkoxide precursor (Pre-1) was synthesized as per reaction scheme mentioned below:

$$Mg + xC_2H_5OH + yCH_3OH \xrightarrow{I_2} Mg[(OC_2H_5)_x(OCH_3)_y] + H_2$$

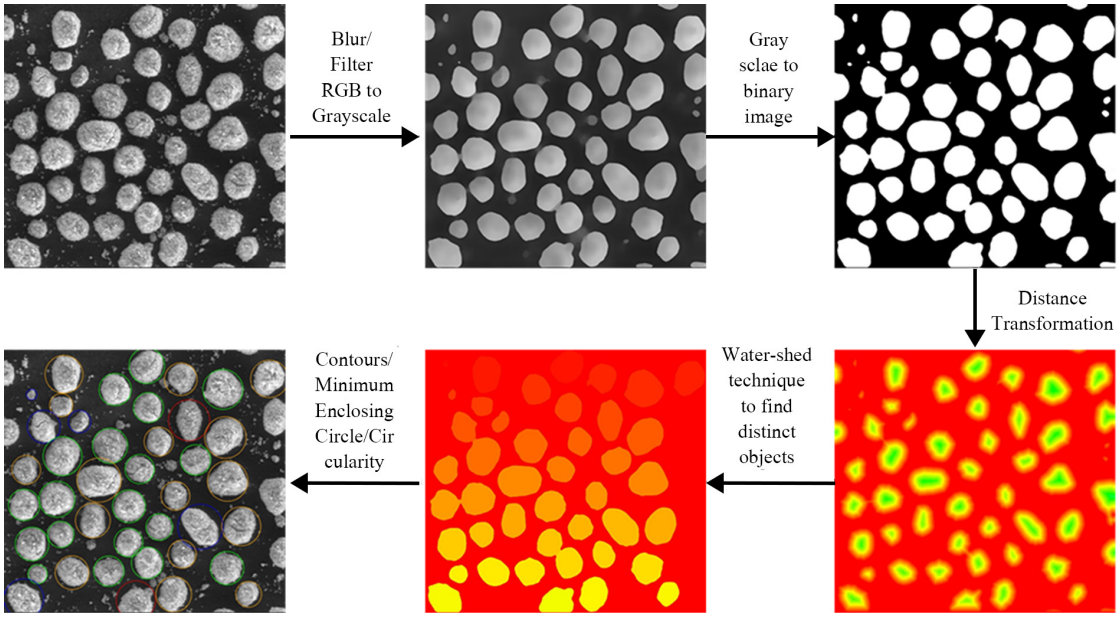

Figure 2. Steps followed in circularity of particles analysis as indicated by arrows linking the images before and after processing.

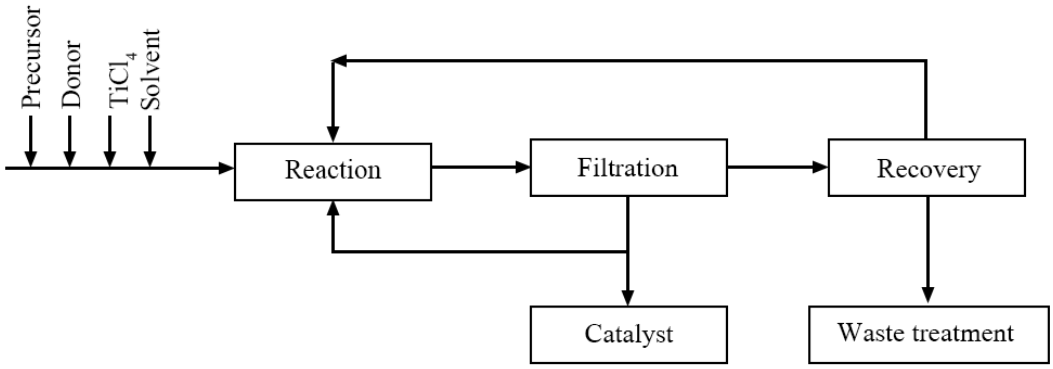

Figure 3. Process flow diagram for catalyst synthesis.

where, molar ratio of x and y is in the range of 10-12. It is characterized for composition and physical characteristics. The results are mentioned in below in Table 1. It is having 76.8% alkoxy and 22.3% magnesium. Its narrow particle size distribution is indicated by span of 0.83.

Catalyst (Cat-1) synthesized using above mentioned magnesium alkoxide precursor by the process mentioned in Figure 3, was characterized for its composition and physical characteristics. The results are mentioned in Table-2. Titanium is active component of the catalyst, incorporated by treating magnesium alkoxide with titanium tetrachloride. Diisobutyl phthalate is used as an internal donor in the catalyst. The produced catalyst is having 2.9% titanium and 10.1% internal electron donor. Similar catalyst composition is also reported by Chumachenko *et al.,* [21] while synthesizing Ziegler-Natta catalyst at 110°C in chlorobenzene solvent. The internal donor (diisobutyl phthalate) and Ti content have been reported to vary with reaction temperature and solvent used.

There is broadening of particle size distribution, as compared to that of catalyst. This is due the change in morphological orientation while transition of particles from precursor to catalyst. It is a function of precursor as well as catalyst synthesis process. Our current study is about correlating this transition. Performance of the above catalyst (Cat-1) is evaluated for propylene polymerization in gas phase fluidized bed reactor. Polymerization conditions are temperature of 68-70°C and pressure of 32 kg/cm^2. Triethyl aluminum is used as a co-catalyst and cyclo-hexyl-methyl-dimethoxy-silane based external electron donor is used as a selectivity control agent.

The catalyst shows activity of 14.5 kg.PP/g.cat for propylene polymerization. Catalyst productivity is a function of catalyst characteristics as well as polymerization conditions like temperature, pressure, polymer residence time, etc. The resultant polymer with a stereoregularity of 96.8% was characterized as xylene insoluble fraction. It was controlled by the way of adding selectivity control agent. The melt flow index (MFI), which is an indication of molecular weight was characterized at 230°C temperature and 2.16 kg load. The synthesized polypropylene showed an MFI of 10.6g/10min. Hydrogen was used as a chain terminating agent. The MFI of polymer was controlled by its concentration in a reactor. The data in above table shows increase in MFI with increase in hydrogen concentration in the reactor, due to enhanced chain termination rate. Isotactic index increases with increase in external donor concentration (reduction in

Table 1. Composition and characteristics of precursor.

Composition		Particle Size Distribution				
Alkoxy content (Wt.%)	Mg content (Wt.%)	D_{10}, (Micron)	D_{50}, (Micron)	D_{90}, (Micron)	D_{mean} (Micron)	D_{span}
76.8	22.3	16	24	36	25	0.83

Table 2. Composition and characteristics of catalyst.

Composition				Particle Size Distribution				
Ti (Wt.%)	Mg (Wt.%)	Cl (Wt.%)	DIBP (Wt.%)	D_{10}, (Micron)	D_{50}, (Micron)	D_{90}, (Micron)	D_{mean} (Micron)	D_{span}
2.9	17.6	59.6	10.1	5	25	38	24	1.32

Table 3. Propylene polymerization performance.

Al/D, Molar Ratio	Isotactic Index (Wt.%)	H_2/C_3, Molar Ratio	MFI (g/10 min)	Activity (kg PP/g cat)
2.5	97.0	0.006	3.3	15.4
2.8	96.9	0.013	10.1	15.8
2.7	96.5	0.014	11.5	16.4

Al/D ratio). External donor blocks atactic sites, but some of the isotactic sites also gets blocked at higher concentration. It results into reduction in catalyst activity, as can be seen in above table. Isotactic index and catalyst activity are inversely related. The polymer resin showed an average particle size of 560 microns and a tapped bulk density of 0.39g/cc. Polypropylene resin bulk density is one of the critical performance parameters in gas phase polymerization process. It governs the throughput of reactor and is strong function of catalyst particle size distribution.

Precursor to catalyst correlation development

The magnesium alkoxide precursor, the Ziegler-Natta catalyst, and the polymers that use it are produced on a commercial scale. Four batches of respective precursors and catalysts are chosen for studies on morphology correlation while transition from precursor to catalyst. Understanding morphology replication from precursor to catalyst is attempted through evaluation of particle size distribution, circularity distribution and statistical analysis of data, and are mentioned in the following section.

Particle size and its distribution

Particle size of precursor, catalyst, and quantification of its distribution at 10%, 50%, 90% of mass, average particle size and span of particle size distribution are revealed in Figure 4. The catalyst particle size (D_{mean}, D_{50} and D_{90}), and D_{span} are higher than that of precursor, which is consistent with the results of Taniike *et al*., (2013) [33]. Particle size distribution of precursor and catalyst follows similar pattern in all the four set of experiments. Distribution of catalyst particle size broadens as compared to that of precursor, as can be seen from increase in D_{span}. The broadening of particle size is due to fragmentation and agglomeration in

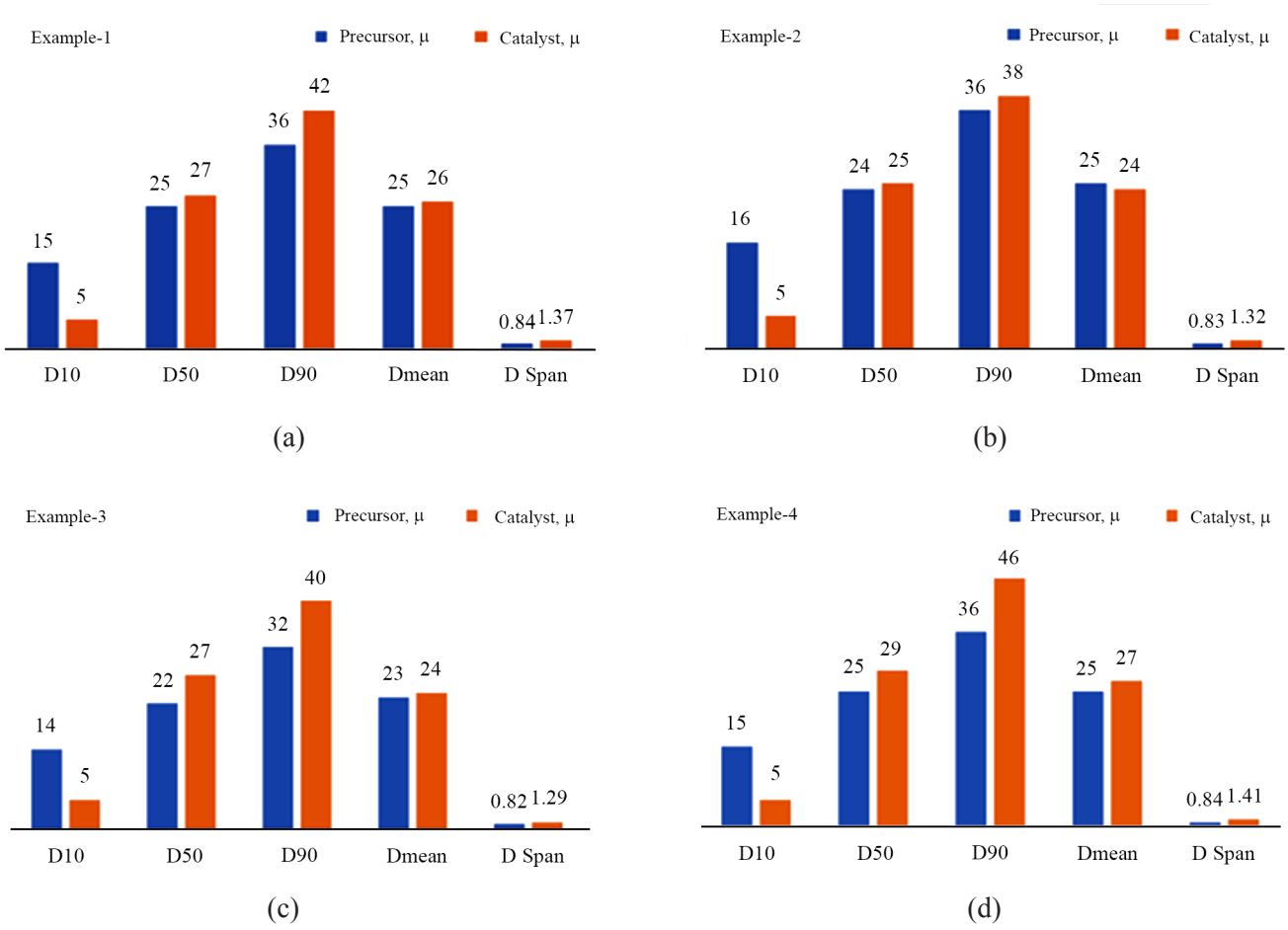

Figure 4. Particle size distribution of precursor and catalyst.

catalyst synthesis process. Increase in particle size (i.e., D_{50} and D_{90}) is due to formation of $(MgCl_2)_n(TiCl_4)_m(DIBP)_o$ complex and also agglomeration [34].

Decrease in D_{10} is due to fragmentation of precursor and could be due to exothermicity of the reaction, as well as shear induced in catalyst manufacturing process [35]. Extent of variation in D_{90} and D_{span} in Example 4 is higher, signifying more agglomeration. On the other-hand Example-3 shows smaller variation. Similar results are also reported by Klaue *et al*., [36]. They reported increased catalyst fragmentation at enhanced shear in catalyst manufacturing process, as can be seen from increased polymer to catalyst particle size ratio.

Morphology determination of precursor, catalyst, and polymer

Figure 5 shows particle morphology of precursor, catalyst, and polymer. Precursor particles are found to have near to spherical morphology, distinctly separated particles from each other and contains no agglomerates or fines. Visually, the catalyst produced using these precursors also shows spherical shape particles, with marginally higher size. But there are some small particles (fines) around catalyst, indicating fragmentation while catalyst synthesis. This is also confirmed by reduction in catalyst particle size at 10% population (i.e., D_{10}) compared to precursor. Extent of fragmentation and agglomeration in catalyst is more in case of Example-4, same is also confirmed by increase in D_{span} to 1.41. Similar observations are also reported by Zohuri *et al.,* [37-38] for the synthesis of $SiO_2/MgCl_2$ catalyst for synthesizing of ultra-high molecular weight polyethylene. They investigated morphology of these catalysts by SEM and observed broken particles in the catalyst. The spherical morphology of the support was deteriorated during the catalyst preparation due to strenuous reaction between the supports in reaction conditions. Jamjah *et al*., [39] reported synthesis of $MgCl_2$.nEtOH adduct (precursor) through emulsion process, supported $TiCl_4$ catalyst using it for ethylene polymerization. They evaluated morphology through SEM, and reported morphology replication from precursor to catalyst, but this process is different from the one adopted in the current studies.

The impact of catalyst fragmentation and agglomeration is clearly visiblfe on the polymer morphology. It is lesser in case of Example-2, as can be seen from closer catalyst particle size at 10%, 50% and 90% population (i.e., D_{10}, D_{50} and D_{90}) compared to precursor. The polymer produced using catalyst of Example-2 shows spherical morphology resin. Whereas few flakes like polymer morphology particles are observed in case of Example-1, 3 and 4, which is the result of agglomerated catalyst particles.

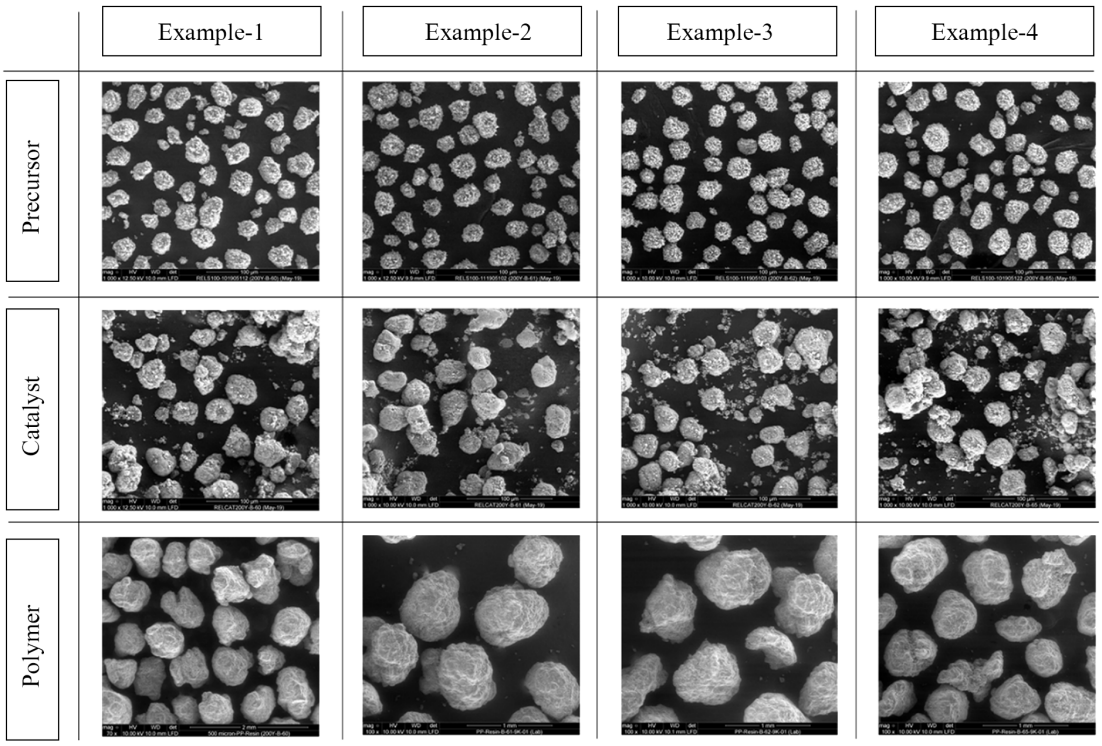

Figure 5. Morphology of precursor and catalyst by SEM.

This agglomeration is indicated by increase in catalyst particle size at 90% population (i.e., D_{90}) compared to precursor. Munoz-Escalona *et al.,* [40] reported similar observation of replication of polymer morphology to that of catalyst. They observed improvement in morphology after grinding of the catalyst, due to deagglomeration. It resulted into morphological polymer, as compared to that of non-grinded catalyst.

Circularity of precursor and catalyst batches

Morphology of the precursor and catalyst particle can be determined from two-dimensional shape by circularity analysis, where we assume circularity to be an analogous metric of sphericity in three dimensions. Although we realize that this is a severe simplifying approximation which in reality would not be true, our objective here is to examine the usefulness of circularity as a metric for studying particles. Since this is statistical investigation, correctness of the results depends on sample size. For more accuracy, the maximum number of samples should be selected. If an enclosing or circumscribing circle that just touches the outermost edges of the particle is drawn from the center of each catalyst particle as shown in Figure 6 for Example 1 (Catalyst), the ratio of area of the precursor/catalyst particle to the area of the enclosing circle is calculated and reported as circularity. Figure 6 also shows a sample image of particle overlaid with a rectangular grid. The circularity computed from the computer vision program for specific particles was compared with circularity that can be manually computed by counting the individual grid block areas that are covered by particular matter (in the image) and suitably approximating the boundaries where the grid block is partially covered by particulate matter. The grid block areas thus counted and added can then be divided by the enclosing circle area to obtain a manually determined circularity value, that is compared with the machine determined circularity value for validation. Table 4 shows this comparison for selected particles from the image.

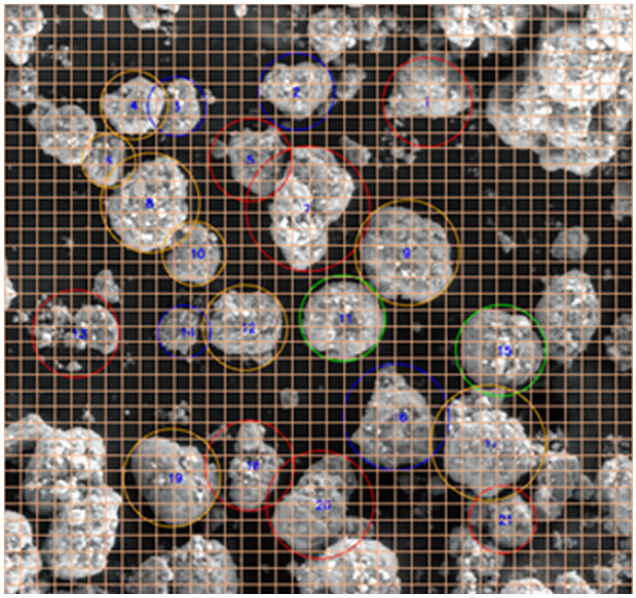

Figure 6. Circularity of selected particles from image (Example 1/catalyst) overlaid with a rectangular grid.

Table 4. Circularity of selected particles from Figure 6 determined manually and by program.

Particle No. in Figure 6	Particle Circularity	
	Manual	Computer Vision based Tool
8	0.768	0.760
9	0.729	0.790
12	0.728	0.747
16	0.593	0.638
18	0.479	0.500

Statistics of the circularity distribution in terms of median circularity is shown in Figure 7.

As can be seen from Figure 7, the median circularity of the precursor is found to be consistently higher, in the range of 0.7±0.03. The median circularity of the catalyst is found to be lower than that of respective precursors in case of all the batches. These observations are in line with visual observations of the particles (from Figure 5) and from our experience as well we note that the precursor particles consistently display a more spherical morphology as compared to catalyst particles at a preliminary level, these results show the possibility of developing circularity distributions as a useful quality parameter to characterize sphericity of catalyst particles produced. Our observations are also in line with Taniike *et al.*, in 2013, who reported decrease in circularity in catalyst as compared to

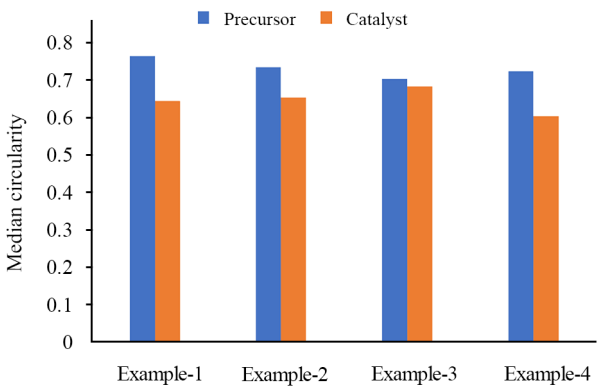

Figure 7. Median circularity of precursor and catalyst.

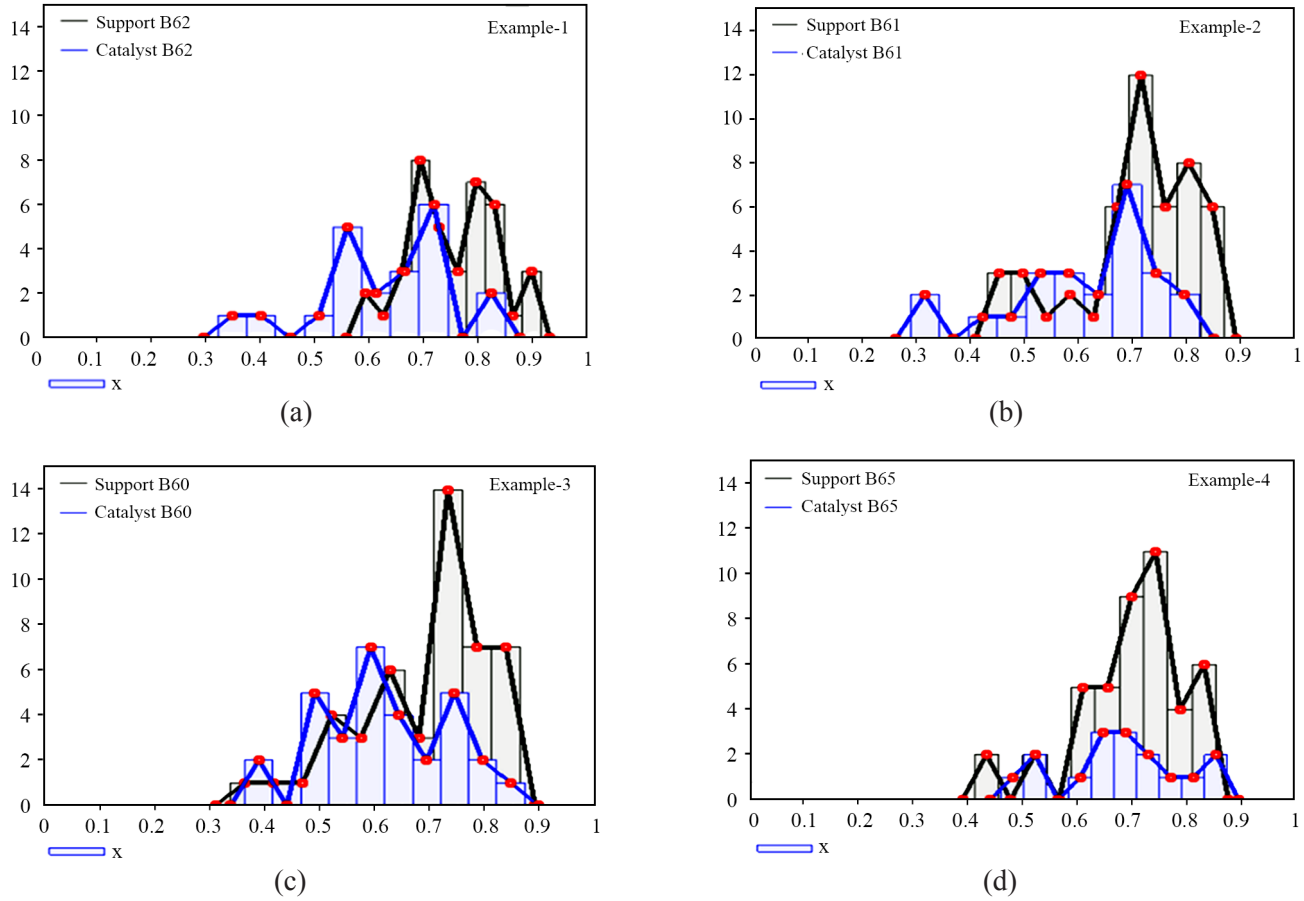

Figure 8. Circularity distribution of precursor and catalyst.

precursor [40]. The decrease in morphology during the transfer of particles from the precursor to the catalyst may be due to the aggregation conditions (i.e. higher reaction rate, shear inside the reactor and shear during the transfer of the catalyst from one vessel to another vessel) in the catalyst synthesis process. Further studies are planned to verify these observations.

Figure 8 shows circularity distribution of the precursor and catalysts, wherein the frequency of occurrence is plotted against circularity distribution. The circularity distribution curve of catalyst shifts to left side of the X axis in the Figure, indicating deterioration of morphology towards lower values of (less perfect) circularity as compared to that of the distribution curve for the corresponding precursor. The extent of variation in catalyst circularity is higher, which may be due to batch-to-batch variation in process conditions. Circularity analysis through computer vision approach gives a useful approximation to study SEM images and the circularity can be regarded as a first approximation to the particle sphericity. The circularity changes as detected by the computer vision technique can be used as a basis to quantify in future the replication of morphology from precursor to catalyst and screen the batches for using in polymerization.

CONCLUSION

A complete process from precursor and Ziegler Natta catalyst from developed precursor is studied. This catalyst used propylene polymerization through gas phase process, and the effect of polymerization conditions on polymer characteristics was evaluated. Morphology variation studies are carried out upon transitioning precursor to catalyst. Precursor and catalyst morphology was characterized through SEM at similar resolution level. A simplified approximation of sphericity (3-dimensional) to that of circularity (2-dimensional) is assumed in this study. Computer vision approach is used for converting qualitative data (i.e., morphology) to the quantitative number (i.e., circularity). Also, particle size distribution variation studies are carried out to endorse the observations. Particle size distribution studies shows that there is a reduction in D_{10} and an increase in D_{90} in

catalyst synthesis process. It is due to fragmentation and agglomeration of catalyst particles. Particle fragmentation and agglomeration can also be observed from the changes in morphology. The synthesized catalyst showed a reduction in circularity, which was correlated with its morphology. These studies show that circularity can provide a quantitative reflection on morphology.

The quantification of morphology and its correlation with process parameters in the manufacturing process is important. Thus, computer vision-based tool can become important in the quantification and correlations development, as well as screening catalyst batches for commercial usage.

ACKNOWLEDGEMENTS

The authors would like to acknowledge Reliance Industries Limited (RIL) for providing resources to carry out this work.

CONFLICTS OF INTEREST

The authors declare that they have no conflicts of interest.

REFERENCES

1. Hutchinson RA, Chen CM, Ray WH (1992) Polymerization of olefins through heterogeneous catalysis X: Modeling of particle growth and morphology. J Appl Polym Sci 44: 1389-1414
2. Grof Z, Kosek J, Marek M, Adler PM (2003) Modeling of morphogenesis of polyolefin particles: Catalyst fragmentation. AIChE J 49: 1002-1013
3. Kissin YV, Nowlin TE, Mink RI, Brandoloni AJ (2000) A new cocatalyst for metallocene complexes in olefin polymerization. Macromolecules 33: 4599-4601
4. Chumachenko NN, Zakharov VA, Bukatov GD, Sergeev SA (2014) A study of the formation process of titanium-magnesium catalyst for propylene polymerization. Appl Catal-A 469: 512-516
5. Fisch AG (2023) Fragmentation-oriented design of olefin polymerization catalysts: Support porosity. Catalysts 13: 160-168
6. Hutchinson RA, Ray WH (1991) Polymerization of olefins through heterogeneous catalysis. IX. Experimental study of propylene polymerization over a high activity $MgCl_2$-supported Ti catalyst. J Appl Polym Sci 43: 1271-1285
7. Wristers J (1973) Nascent polypropylene morphology: Polymer fiber. J Polym Sci Pol Phys 11: 1601-1617
8. Chen Y, Liu XG (2005) Modeling mass transport of propylene polymerization on Ziegler–Natta catalyst. Polymer 46: 9434-9442
9. Harshe YM, Utikar RP, Ranade VV (2004) A computational model for predicting particle size distribution and performance of fluidized bed polypropylene reactor. Chem Eng Sci 59: 5145-5156
10. Spitz R, Bobichon C, Guyot A (1989) Synthesis of polypropylene with improved $MgCl_2$-supported Ziegler-Natta catalysts, including silane compounds as external bases. Macromol Chem Phys 190: 707-716
11. Guastalla G, Giannini U (1983) The influence of hydrogen on the polymerization of propylene and ethylene with an $MgCl_2$ supported catalyst. Makromol Chem Rapid Commun 4: 519-527
12. Samson JJC, Middelkoop BV, Weickert G, Westerterp KR (1999) Gas phase polymerization of propylene with a highly active Ziegler-Natta catalyst. AIChE J 45: 1548-1558
13. Cancelas AJ, Monteil V, McKenna TFL (2016) Influence of activation conditions on the gas phase polymerisation of propylene. Macromol Symp 360: 133-141
14. Liu B, Matsuoka H, Terano M (2001) Stopped-flow techniques in Ziegler-catalysis. Macromol Rapid Commun 22: 1–24
15. Martino AD, Broyer JP, Schweich D, Bellefon CD, Weickert G, McKenna TFL (2007) Design and implementation of a novel quench flow reactor for the study of nascent olefin polymerisation. Macromol React Eng 1: 284-297
16. Poonpong S, Dwivedi S, Taniike T, Terano M (2014) Structure-performance relationship for di-alkyl dimethoxy silane as external donor in stopped-flow propylene polymerization using Ziegler-Natta catalyst. Macromol Chem Phys 215: 1721-1727
17. Olalla B, Broyer JP, McKenna TFL (2008) Heat transfer and nascent polymerisation of olefins on

supported catalysts. Macromol Symp 271: 1-7
18. McKenna TFL, Tioni E, Ranieri MM, Alizadeh A, Boisson C, Monteil,V (2013) Catalytic olefin polymerisation at short times: Studies using specially adapted reactors. Can J Chem Eng 91: 669-686
19. Mori H, Ohnishi K, Terano M (1998) Multiplicity of molecular weight distribution of polyethene produced with modified-polypropene-supported Ziegler catalyst systems. Macromol Chem Phys 199: 393-399
20. Arabi H, Abedini H, Dolatshahi H, Nejabat GR (2013) Ziegler-Natta catalyst preparation process: Influential parameters on particles morphology and activity of catalyst in propylene polymerization. Iran J Polym Sci Technol 26: 209-219
21. Chumachenko NN, Vladimir A, Zakharov SA, Cherepanova SV (2017) Effect of the synthesis conditions of titanium-magnesium catalysts on the composition, structure and performance in propylene polymerization. Polyolefin J 4: 111-122
22. Redzic E, Garoff T, Mardare CC, List M, Hesser G, Mayrhofer L, Hassel AW, Paulik C (2016) Heterogeneous Ziegler–Natta catalysts with various sizes of $MgCl_2$ crystallites: synthesis and characterization. Iran Polym J 25: 321-337
23. Alizadeh A, McKenna TFL (2018) Particle growth during the polymerization of olefins on supported catalysts. Part 2: Current experimental understanding and modeling progresses on particle fragmentation, growth, and morphology development. Macromol React Eng 12: 1700027
24. Ermakov YI, Zakharov VA (1972) Determination of the number of active centres and growth rate constants in the catalytic polymerisation of α-alkenes. Russ Chem Rev 41: 203-215
25. Nagel EJ, Kirillov VA, Ray WH (1980) Prediction of molecular weight distributions for high-density polyolefins. Ind Eng Chem Prod Res Dev 19: 372-379
26. Trivedi PM, Gupta VK (2021) Progress in $MgCl_2$ supported Ziegler-Natta catalyzed polyolefin products and applications. J Poly Res 45: 02412-5
27. Makwana U, Naik DG, Singh G, Patel V, Patil HR, Gupta VK (2009) Nature of phthalates as internal donors in high performance $MgCl_2$ supported titanium catalyst. Catal Lett 131: 624-631
28. Makwana UC, Singala KJ, Patankar RB, Singh SC, Gupta VK (2012) Propylene polymerization using supported Ziegler-Natta catalyst systems with mixed donors. J Appl Polym Sci 125: 896-901
29. Sharma A, Singh S, Singh G, Gupta VK (2011) Polypropylene resin flowability improvement through catalyst morphology. Polym Plast Tech Eng 50: 418-422
30. Gupta VK, Singh S, Makwana UC, Joseph J, Singala KJ, Rajesh S, Patel V, Yadav MK, Singh G (2014) Spheroidal particles for olefin polymerization catalyst. US8633124B2
31. Gupta VK, Patil HR, Naik DG, Kaur S, Singh G, Vyas PB (2011) Catalyst system for polymerization of olefins. US8043990 B2
32. Gupta VK, Patil HR, Naik DG (2014) Propylene polymerization catalyst system. US8853118B2
33. Taniike T, Funako T, Terano M (2014) Multilateral characterization for industrial Ziegler-Natta catalysts toward elucidation of structure-performance relationship. J Catal 311: 33-40
34. Zorve P, Linnolahti M (2018) Adsorption of titanium tetrachloride on magnesium dichloride clusters. ACS Omega 3: 9921-9928
35. Abboud M, Denifl P, Reichert KH (2005) Study of the morphology and kinetics of novel Ziegler-Natta catalysts for propylene polymerization. J Appl Polym Sci 98: 2191-2200
36. Klaue A, Kruck M, Friederichs N, Bertola F, Wu H, Morbidelli M (2019) Insight into the synthesis process of an industrial Ziegler-Natta catalyst. Ind Eng Chem Res 58: 886-896
37. Zohuri G, Bonakdar MA, Damavandi S, Eftekhar M, Askari M, Ahmadjo S (2009) Preparation of ultra high molecular weight polyethylene using bi-supported $SiO_2/MgCl_2$(spherical)/$TiCl_4$ Catalyst: A morphological study. Iran Polym J 18: 593-600
38. Zohuri GH, Askari M, Ahmadjo S, Damavandi S, Eftekhar M, Bonakdar MA (2010) Preparation of ultra-high-molecular-weight polyethylene and its morphological study with a heterogeneous Ziegler–Natta catalyst. J Appl Polym Sci 118: 3333-3339
39. Jamjah R, Zohuri GH, Vaezi J, Ahmadjo S, Nekomanesh M, Pouryari M (2006) Morphological study of spherical $MgCl_2$.nEtOH

supported $TiCl_4$ Ziegler-Natta catalyst for polymerization of ethylene. J Apply Polym Sci 101: 3829-3834

40. Munoz-Escalona A, Alarcon C, Albornoz LA, Fuentes A, Sequera JA (1988) Morphological characterization of Ziegler-Natta catalysts and nascent polymers. In: Transition metals and organometallics as catalysts for olefin polymerization, eds: Kaminsky W, Sinn H, Springer, Berlin, Heidelberg